Ultrasonics 72 (2016) 24–33

Contents lists available at ScienceDirect

Ultrasonics

journal homepage: www.elsevier.com/locate/ultras

An ultrasonic orthopaedic surgical device based on a cymbal transducer

Fernando Bejarano [a], Andrew Feeney [a], Robert Wallace [b], Hamish Simpson [b], Margaret Lucas [a,*]

[a] School of Engineering, University of Glasgow, Glasgow G12 8QQ, UK
[b] School of Clinical Sciences, University of Edinburgh, Edinburgh EH16 4SB, UK

ARTICLE INFO

Article history:
Received 19 April 2016
Received in revised form 8 July 2016
Accepted 8 July 2016
Available online 12 July 2016

Keywords:
Ultrasonic surgical device
Cymbal transducer
Orthopaedic surgery

ABSTRACT

An ultrasonic orthopaedic surgical device is presented, where the ultrasonic actuation relies on a modification of the classical cymbal transducer. All current devices consist of a Langevin ultrasonic transducer with a tuned cutting blade attached, where resonance is required to provide sufficient vibrational amplitude to cut bone. However, this requirement restricts the geometry and offers little opportunity to propose miniaturised devices or complex blades. The class V flextensional cymbal transducer is proposed here as the basis for a new design, where the cymbal delivers the required vibrational amplitude, and the design of the attached cutting insert can be tailored for the required cut. Consequently, the device can be optimised to deliver an accurate and precise cutting capability. A prototype device is presented, based on the cymbal configuration and designed to operate at 25.5 kHz with a displacement amplitude of 30 μm at 300 V. Measurements of vibrational and impedance responses elucidate the mechanical and electrical characteristics of the device. Subsequent cutting tests on rat femur demonstrate device performance consistent with a commercial Langevin-based ultrasonic device and show that cutting is achieved using less electrical power and a lower piezoceramic volume. Histological analysis exhibits a higher proportion of live cells in the region around the cut site for the cymbal device than for a powered sagittal or a manual saw, demonstrating the potential for the ultrasonic device to result in faster healing.

1. Introduction

Ultrasonic cutting devices have been developed for use in a number of orthodontic and surgical procedures, for example in oral prophylaxis [1], periodontics [2], and soft [3] and hard [4] tissue dissections. The increasing number of surgeons adopting ultrasonic devices has increased the demand for devices capable of procedures where delicate tissue structures must be protected, and at surgical sites that are difficult to access. This presents challenges in design for miniaturisation and for the incorporation of more complex geometries. Currently, ultrasonic surgical devices most commonly consist of a Langevin piezoelectric transducer with an insert, such as a cutting blade, attached, where both the transducer and cutting insert are tuned to resonate in a longitudinal mode at a low ultrasonic frequency, usually in the 20–60 kHz range. Langevin transducers incorporate a stack of piezoceramic discs or rings, and a Langevin-type device must be in resonance to achieve sufficient ultrasonic displacement amplitude at the cutting tip, usually in the order of several tens of microns. The requirement for resonance places design constraints on the geometry of ultrasonic devices. For longitudinal-mode resonance, the device geometry must be a multiple of a half-wavelength at the operating frequency. If required, combined longitudinal-flexural [5] or longitudinal-torsional [6] motions of the cutting tip can be introduced through features such as slits in the transducer and/or cutting insert and curved cutting inserts, and this motion can be further controlled by the proximity of features to nodal locations. The cutting insert itself must incorporate amplitude gain, usually achieved through increasing the slenderness of the device towards the cutting tip, but this can result in stress concentrations, causing failure of the insert, and motion consisting of multiple modes of vibration through the excitation of nonlinear responses [7]. There is hence an opportunity to design ultrasonic orthopaedic devices for a much wider range of bone cutting procedures, if the actuation of the transducer alone can excite sufficient ultrasonic amplitude, for example in the order of tens of microns, such that there is no need for the cutting insert to be in resonance. One such potential transducer is the class V flextensional transducer, known as a cymbal. This study reports on the adaptations of the cymbal transducer in the design of an ultrasonic orthopaedic surgical device (UOSD) and on the subsequent characterisation of its performance in comparison with more conventional bone cutting devices. The motivation for the development of the UOSD is to demonstrate that an

* Corresponding author.
E-mail address: Margaret.Lucas@glasgow.ac.uk (M. Lucas).

http://dx.doi.org/10.1016/j.ultras.2016.07.004
0041-624X/

ultrasonic device for orthopaedic surgery based on a cymbal transducer can deliver comparable or improved cutting in bone at low electrical power and with lower volume of piezoelectric material than a device based on a Langevin transducer, and that the device can cut successfully without tuning the cutting insert.

1.1. Ultrasonics in bone surgery

The first attempt to introduce ultrasonic technology into bone cutting procedures was a drilling device for dentistry [8]. However, subsequent applications of ultrasonics in dentistry have principally concentrated on dental scaling. A number of inventions by Balamuth formed the foundation for developments in this field. The first of these inventions was a cutting device which incorporated an abrasive slurry [9]. The original device comprised an outer casing with an enclosed magnetostrictive transducer which was connected to a mechanical amplifier, known as a horn. The horn was secured at one end of the laminated stack of magnetostrictive material, and a threaded end-section allowed for connection of a cutting insert to the horn. During cutting, the abrasive slurry was applied directly to the bone surface. The device possessed an external flexible sheath, which contained capillary tubing for abrasive slurry delivery to the cut site and also provided cooling for the transducer.

However, it was not until 2001 that the first ultrasonic device for bone surgery procedures was commercialised, called Piezosurgery® [10,11]. Although there is half a century of research and technological advances between the early invention of Balamuth and the launch of the Piezosurgery® device, the basic design elements have remained largely unchanged, with the exception of the replacement of the magnetostrictive material with piezoelectric ceramics. The Piezosurgery® device comprises a Langevin transducer incorporating a stack of four PZT rings under compression which are coupled to a horn with a threaded end to enable the attachment of different cutting inserts. Inside the transducer body, a tube is introduced, running parallel to the compression bolt, to deliver coolant directly to the cutting tip. The coolant controls the temperature of both the transducer and the cutting site, and also irrigates the cutting site. The Piezosurgery® device operates at a frequency in the range 24–36 kHz. The piezoceramic stack, transducer horn and cutting insert generate micro-vibrations which have a displacement amplitude between 60 μm and 210 μm, depending on which cutting insert is attached, and the designated electrical input power. The device is able to cut mineralised tissue whilst avoiding damage to surrounding neurovascular and other soft tissues, and delicate connective tissue structures, thereby ensuring enhanced precision and visibility and maintaining a blood-free surgical site.

1.2. The cymbal transducer

Although commercial ultrasonic cutting devices have been adopted for a range of surgical procedures, particularly in oral and maxillofacial surgeries, the limitation of the requirement for resonance can restrict the development of new designs. The cymbal transducer is a type of flextensional transducer that was evolved in the 1990s from the moonie transducer [12]. This class V flextensional transducer consists of a piezoceramic disc, poled in the thickness direction, sandwiched between two dome-shaped metal shell end-caps. The resonance frequency of the transducer is dependent on the material properties of the end-caps and their dimensions [13]. Each end-cap possesses a cavity which enables the structure to behave as a mechanical transformer, converting the radial motion of the piezoceramic disc into axial-flexural motion of the end-caps. The mechanical coupling between the piezoceramic disc and the metal end-caps is formed by an epoxy resin. This material acts as a bonding agent, meaning that the conversion of the radial displacement of the piezoceramic to the flexural displacement of the end-caps relies on the formation and strength of this bond.

1.3. Modification of the cymbal for power ultrasonic applications

The mechanical coupling is a limitation for the application of the cymbal transducer in power ultrasonic devices [14–16], where the epoxy resin bond layer is known to fail under ultrasonic vibration. In an attempt to address this, an adaptation of the classical cymbal (CCym) transducer design was fabricated [17], based on the improved cymbal transducer proposed by Lin [16]. This transducer incorporates a piezoceramic disc which is coupled with a metal ring, and fixed with bolts to two end-caps. A high-strength epoxy resin is used to reinforce the mechanical coupling to the piezoceramic disc. This coupling between the end-caps and the piezoceramic disc enables the device to be driven at much higher excitation levels than the CCym transducer. For example, it has been demonstrated that a CCym can be driven at 40 V with a displacement amplitude of approximately 50 μm prior to failure, compared to a displacement amplitude of 90 μm at 100 V for the improved transducer [17]. This displacement amplitude is achievable with the improved transducer, since the mechanical coupling does not rely on the integrity of the epoxy bond layer. Furthermore, the experimental characterisation results of this improved transducer demonstrate that even though the transducer incorporates additional assembly complexity, by the inclusion of threaded bolts and a metal ring, the cavity resonance mode of the transducer matches that of the CCym.

Importantly, for the design of orthopaedic devices, when a metal bar was attached to an end-cap, the displacement amplitude was largely independent of the mass of the bar within the range of masses studied, from 0.39 to 1.48 g, a range that is consistent with small bone cutting blades [18]. Based on the improved transducer, a new configuration was developed for use in power ultrasonic applications [17], referred to as the single output face cymbal transducer (SOFCym), for operation with electrical power of at least 50 W. In this configuration, one of the end-caps is replaced by a supporting back-shell as shown in Fig. 1. A preliminary study of an ultrasonic cutting device based on the SOFCym, which was focussed on transducer design, demonstrated that it could be used to cut bone in ex vivo conditions [19]. This research is extended here to perform design and experimental characterisation of the device and bone-cutting trials. The UOSD under investigation is designed to operate at 25 kHz, which lies within the range of resonance frequencies (typically 20–30 kHz) of commercial ultrasonic surgical devices. By miniaturising the device, there is potential for delicate orthopaedic surgeries to be performed, with less tissue damage, as minimally invasive procedures.

2. Design and fabrication

The schematic of a CCym is shown in Fig. 1(a), where two identical metal end-caps are bonded to a piezoelectric ceramic disc. The SOFCym designed for this study, Fig. 1(b), comprises a single titanium (Ti–6Al–4V) end-cap with a threaded stud for cutting insert attachment, a piezoelectric ceramic disc, and a titanium supporting back-shell. In addition to supporting the end-cap, the back-shell houses the piezoelectric element, in this case a piezoceramic disc (PIC-181, PI Ceramic GmbH), and bonding is achieved with an insulating epoxy resin (Eccobond, Ellsworth Adhesives Ltd) which has a lap shear strength of 17 MPa. The dimensions of the SOFCym components are provided in Table 1.

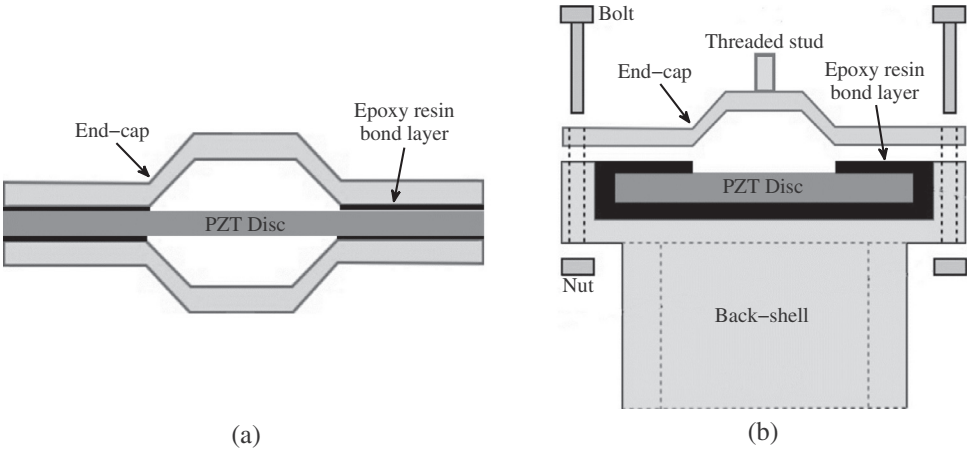

Fig. 1. Transducer assembly schematics, showing (a) the CCym, and (b) the SOFCym.

Table 1
Dimensions of the SOFCym components.

Component	Parameter	Dimension (mm)
End-cap	Total diameter	33.0
	Cavity base diameter	11.0
	Cavity apex diameter	6.0
	Cavity depth	1.0
	Thickness	1.1
	Threaded stud length	5.0
	Threaded stud diameter	3.5
Back-shell	Flange diameter	33.0
	Flange cavity diameter	29.0
	Flange thickness	4.5
	Flange cavity depth	3.4
	Support height	10.0
	Support diameter	22.0
	Support cavity diameter	18.0
Piezoceramic disc	Diameter	27.0
	Thickness	3.0

In the SOFCym configuration, the piezoceramic disc is positioned such that its radial vibration is transferred to the end-cap to generate an axial displacement amplitude with amplification of approximately 40, consistent with a more conventional symmetric two-cymbal transducer [14]. The resonance frequency of the SOFCym is dependent on the dimensions and material properties of the end-cap [20]. The finite element analysis (FEA) software Abaqus was used in the design of the SOFCym, to tune it to the required resonance frequency, and to predict the ultrasonic axial displacement amplitude of the end-cap. To permit different tool attachments, such as a cutting insert, a threaded stud was incorporated on the apex surface of the end-cap as part of this SOFCym design. Once the physical characteristics of the end-cap were defined, a suitable back-shell specification was calculated using FEA. The back-shell geometry is critical for preventing bending stress in the piezoceramic disc and ensuring a uniform piezoceramic disc motion. The material selected for the end-cap and back-shell was titanium (Ti–6Al–4V), due to it being reported to be an ideal horn material based on its acoustic properties [18,21], and stainless steel was used for the bolts and nuts.

A thread-mill machine was used to cut the end-cap shape from titanium bar. Electrical leads were then soldered (Multicore® 309™, with a melting temperature of 180 °C for under 3 s) to the flat surfaces of the piezoceramic disc. The Curie temperature of the ceramic is 330 °C, and so a solder process should employ temperatures that avoid damage or depolarisation of the piezoceramic. Soldering can be conducted at temperatures between 200 °C and 300 °C for PZT types including PIC-181 (Morgan Technical Ceramics). After the solder process, the electrical leads were guided through holes in the back-shell. The piezoceramic disc was located in the flange cavity, after which Eccobond epoxy resin, at a ratio of three parts epoxy resin to one part resin hardener, was deposited and cured at room temperature for 24 h, to form an isolating bond layer. Insulating epoxy resin was used to ensure no short-circuiting, for example between the electrodes and the back-shell, but also because it is known to be stronger than conductive types [14], and this is beneficial for operating at the amplitudes of vibration associated with ultrasonic bone cutting, which are 60–210 μm in lateral motion, and 20–60 μm in vertical motion [4,22]. A layer of epoxy resin was also deposited between the piezoceramic disc and the end-cap, providing additional mechanical coupling, before the end-cap was finally bolted in place. For the UOSD, the aim was for the resonance frequency of the SOFCym with an attached cutting insert to be 25.5 kHz, with the UOSD tailored to deliver 30 μm of axial displacement, sufficient to cut bone, for a 300 V input voltage, which corresponds to an electrical power of 30 W.

3. Characterisation of the UOSD

Characterisation and analysis of the vibration behaviour of the SOFCym with (as a UOSD) and without an attached cutting insert were carried out. Experimental modal analysis (EMA), in part reported in [19], was completed here using a 3-D laser Doppler vibrometer (Polytec CLV). Electrical impedance analysis (Agilent 42942A Impedance/Gain Phase Analyzer) and power harmonic characterisation using a 1-D laser Doppler vibrometer (Polytec CLV) were also performed.

For these experiments, a range of Mectron Piezosurgery® cutting inserts were attached to the SOFCym, and these are shown in Fig. 2. For the subsequent tests of the UOSD, the Piezosurgery® OT7 was used. The OT7 is one of a set of interchangeable inserts used in bone cutting procedures. The shape is designed to deliver an elliptical cutting motion at the cutting edge, with the insert as a whole exhibiting a combined axial-flexural oscillatory motion, such that the ultrasonic cutting tip amplitude can reach 210 μm [4], for an amplitude of under 20 μm of the Langevin transducer. The OT7 was therefore adopted for the UOSD in this study, exhibited in Fig. 3, to test the SOFCym transducer connected to a commercial cutting blade.

The dominant mode of a cymbal transducer is its first cavity mode which, for an ideal transducer, exhibits a uniform displacement amplitude at the apex surface. For a standard cymbal transducer, which has two end-caps, this mode is also known as the

Fig. 2. Hard tissue cutting inserts (Mectron S.p.A.), from left to right: OT7, PS1, OT6 and OT2.

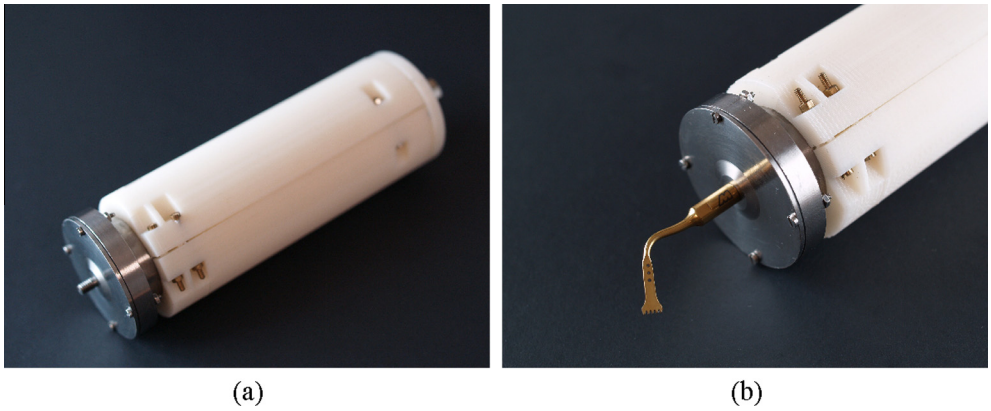

Fig. 3. The SOFCym (a) without the OT7 insert, and (b) with the OT7 insert attached [19].

symmetric mode, because the two end-caps oscillate in an identical synchronous motion and out-of-phase with each other. Achieving this symmetric motion relies on the quality and symmetry achieved in the fabrication of the transducer. For the new SOFCym, the single end-cap must also exhibit amplitude uniformity on the apex surface, but for this transducer, the amplitude uniformity relies on the design of the back-shell, which prevents flexure of the piezoceramic disc.

The mode shapes of the SOFCym and the UOSD were predicted using FEA, and measured using EMA, the results of which are shown in Fig. 4 [19]. In the EMA, a 3-D laser Doppler vibrometer was used in conjunction with a data acquisition system (DataPhysics SignalCalc), and the measured frequency response functions were curve-fitted (ME'ScopeVES), to allow extraction of the modal frequencies and mode shapes. The results demonstrate that the design of a UOSD that is based on a cutting insert not tuned to resonance requires the cymbal transducer to be tuned at a much higher frequency than the final operating frequency of the whole UOSD. In this case, the measured dominant cavity mode resonance of the SOFCym transducer is at 46.2 kHz. Unlike devices at resonance based on Langevin transducers, the cutting insert acts as an added mass connected to the output face of the cymbal end-cap, with the result that the UOSD resonance is at 25.8 kHz, around 20 kHz lower than for the SOFCym itself. Therefore, to ensure that the UOSD will be fabricated to work at the desired operating frequency, the mode of the SOFCym and UOSD, with any connected cutting insert, must be predicted accurately at the design stage by FEA, with the objective that once fabricated, the device operating frequency and mode correlate with that calculated from FEA. Fig. 4 shows that close correlation is achieved between the mode shapes and modal frequencies simulated using FEA and measured using EMA, where the difference between the resonance frequencies of the operational mode obtained from EMA and FEA is 1.9% for the SOFCym and 0.4% for the UOSD. The figure also shows that the OT7 cutting insert maintains its operational longitudinal-flexural motion when connected to the SOFCym. This was achieved by designing the operating frequency of the UOSD to be close to the resonance frequency of the Piezosurgery® inserts, to aim for an effective bone cutting device.

The impedance–frequency response of the SOFCym, with and without the OT7 cutting insert connected, was measured and is shown in Fig. 5. The cavity resonance frequency of the SOFCym was identified at 45.7 kHz and the operational resonance frequency of the UOSD was confirmed as 25.4 kHz.

The effect on the operational frequency of the UOSD as a result of attaching different cutting inserts (and therefore different masses) to the SOFCym is illustrated in Fig. 6, which shows the impedance–frequency spectra measured for the range of

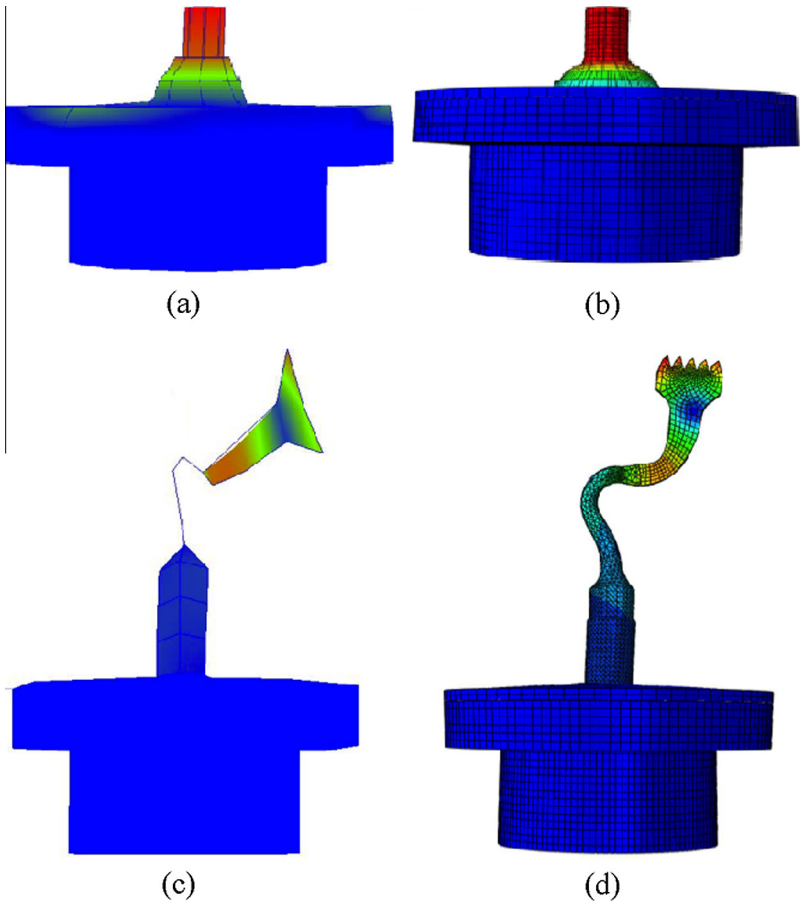

Fig. 4. Vibration mode of the SOFCym at (a) 46170 Hz from EMA and (b) 45282 Hz from FEA, and UOSD with the OT7 cutting insert attached, at (c) 25842 Hz from EMA and (d) 25727 Hz from FEA [19].

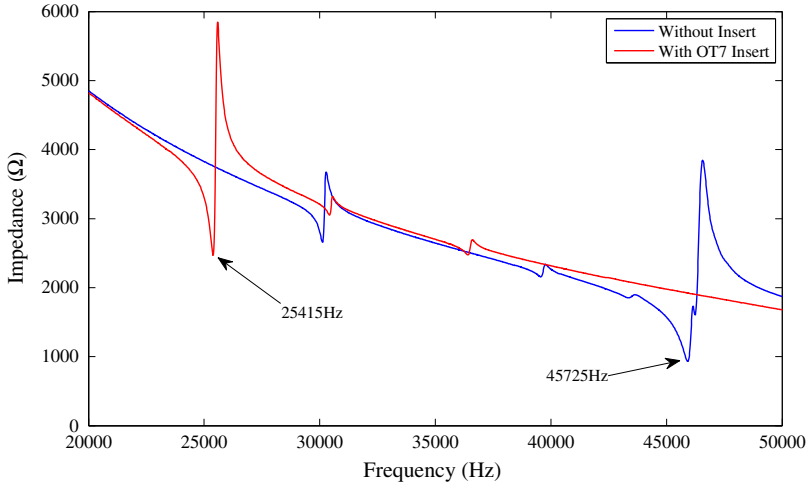

Fig. 5. Impedance–frequency spectra showing the response of the SOFCym without an insert (blue) and UOSD with the OT7 insert attached (red). (For interpretation of the references to colour in this figure legend, the reader is referred to the web version of this article.)

Piezosurgery® inserts pictured in Fig. 2. It is evident that the resonance frequency does not change significantly for inserts of different mass and shape, and stays within a frequency range that can be tracked by commercial ultrasonic surgical device drive platforms. In addition, the UOSD impedance magnitude at the resonance and anti-resonance frequencies is consistent across the different cutting inserts. These results demonstrate that the operational parameters of the UOSD, particularly the device impedance and resonance frequency, are in general independent of the physical characteristics of the cutting insert, within a range of masses and shapes typical of bone cutting inserts.

A power harmonic analysis of the new SOFCym transducer was conducted using a 1-D LDV, where the displacement amplitude of the cymbal end-cap was measured across a 1 kHz frequency range

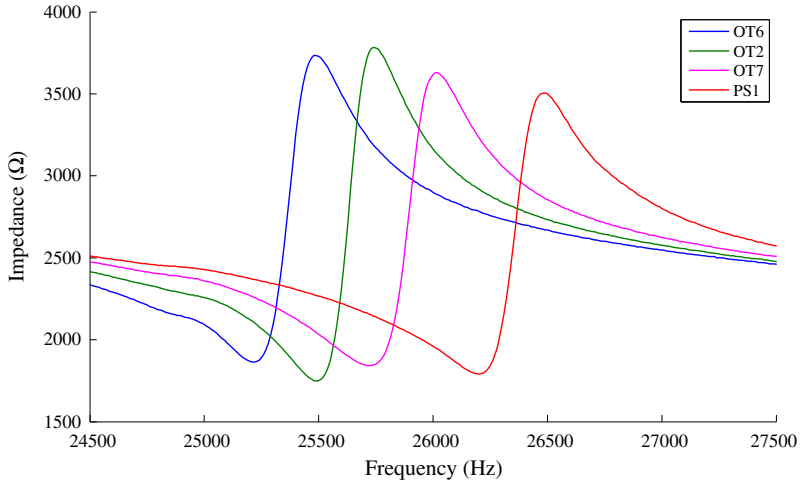

Fig. 6. Impedance–frequency spectra of the UOSD with different cutting inserts.

around its cavity resonance frequency. The harmonic analysis was performed as a sinusoidal excitation at a sweep rate of 0.5 Hz s^{-1} to ensure sufficient resolution to capture any evidence of the jump phenomenon due to non-linear responses. The sweep was also bi-directional, frequency sweep-up followed by frequency sweep-down, so that non-linear responses could be measured and characterised. The results of these measurements, along with the displacement amplitude of the end-cap measured at the cavity resonance frequency, for six input voltages from 3 V to 50 V are shown in Fig. 7.

A resonance peak is exhibited in the displacement amplitude response of the SOFCym at around 45.4 kHz at each input voltage level. Also, the bi-directional sweep data overlaps for each input level, the sweep-up data and sweep-down data coinciding, which demonstrates that there is no unstable region is the vibration response. However, there is evidence of nonlinearity, exhibited here as a decrease in resonance frequency, between 3 V and 30 V, followed by an increase in resonance frequency between 30 V and 50 V, with the 20 V and 30 V response measurements exhibiting as the most symmetrical, indicative of a linear response. A

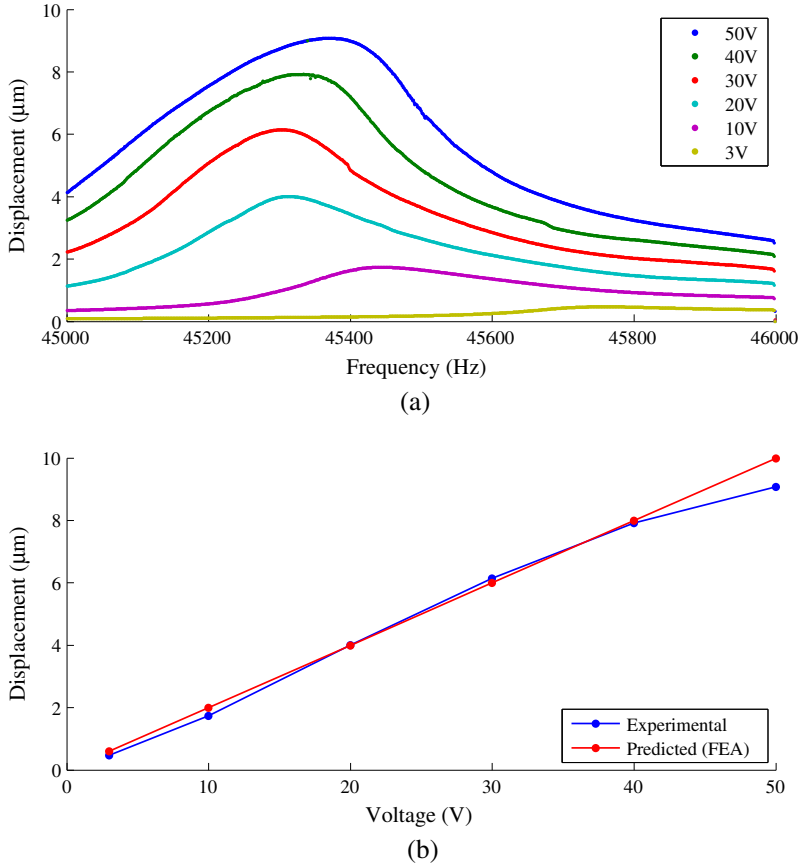

Fig. 7. (a) Displacement amplitude response of the SOFCym, and (b) the relationship between displacement amplitude and input voltage.

decreasing frequency with increasing excitation level is consistent with a softening nonlinear characteristic, whereas an increasing frequency is consistent with a hardening nonlinear characteristic. Nonlinear behaviour can arise from a number of sources. For example, nonlinearity can stem from material properties that are known to be strain-dependent, such as mechanical Q-factor [7], and can also appear as a result of internal dissipation of energy in the piezoceramic causing localised stress and heating [7,17], where piezoceramic properties such as Q-factor and dielectric loss depend on vibration amplitude and temperature. Nonlinear responses can also manifest from other sources such as degradation of the epoxy bond layer [7,17,23]. It is likely in this cymbal transducer that competing dominant material sources are responsible for the change from a softening to hardening behaviour at higher excitation, between 20 V and 40 V, as shown in Fig. 7(a). In the FEA simulation, steady-state dynamic analysis was employed for different input voltages. The results shown in Fig. 7 (b) demonstrate a close correlation between the measured displacement amplitude data and data calculated from FEA.

4. Cutting performance of the UOSD

A rigid polyurethane foam biomechanical mimic test block was used initially to demonstrate the cutting ability of the UOSD, where the cuts were made by the UOSD operating under constant force. First, the power harmonic analysis method was used to measure the relationship between the UOSD (SOFCym plus OT7) electrical input power and the displacement amplitude at resonance. Secondly, the depth of cut achieved for the same power range was measured for a 5-s cutting duration. These results are shown in Fig. 8, where the displacement amplitude was recorded for the UOSD at the base of the OT7 insert, in order to characterise the axial motion. The results in Fig. 8 show that the electrical power of the UOSD with OT7 insert attached increases both with displacement amplitude, from 8.0 μm to 20.9 μm, and depth of cut, from 0.83 mm to 6.97 mm. The cuts in the biomechanical mimic are shown in Fig. 9.

There is an increase in the achievable depth of cut for increasing UOSD electrical input power. The Piezosurgery® device with an OT7 insert, which is based on a Langevin transducer, requires an axial displacement amplitude at the base of the insert of at least 15 μm for effective cutting [4]. For the UOSD, an electrical input power of around 40–50 W is required to achieve this displacement

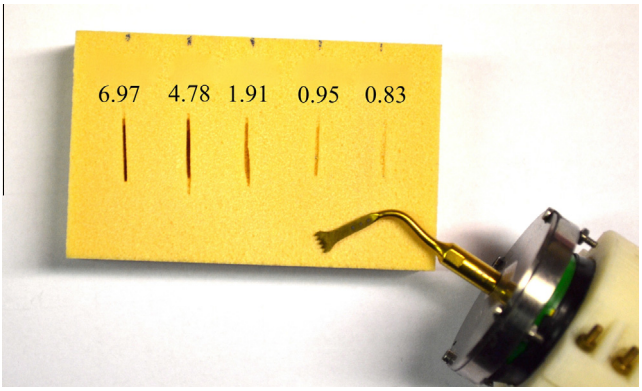

Fig. 9. Depth of cut, in mm, on biomechanical mimic material using the UOSD.

amplitude, as shown in Fig. 8. In comparing the UOSD with the Piezosurgery® device, both can deliver the same ultrasonic displacement amplitude at the cutting tip by applying the same voltage across the piezoceramic, however, only one disc is required for the UOSD whereas four discs are required for the Piezosurgery® device. From analysis of the experimental results and the FEA, the UOSD has the potential to deliver effective cutting with a much smaller transducer and lower piezoceramic volume than its Langevin-based counterpart.

It has been demonstrated that ultrasonic devices used for bone cutting can exhibit higher precision than non-ultrasonic devices such as bone saws and burs, causing less damage to the surrounding soft and hard tissues, and preserving delicate structures such as connective tissue [22]. Ex vivo cutting tests were conducted using the UOSD with the aim of investigating cell death and cell survival around the cut site. For this study, six fresh rat femurs were acquired, each then cut in two separate locations using the UOSD. Two different operational conditions were investigated, the first without any coolant and the second using a coolant liquid, Phosphate Buffered Saline (PBS), which was used at physiological concentration and was applied directly to the cutting site. The UOSD in operation being used to cut a bone specimen is shown in Fig. 10.

Once the bones were cut, they were placed in 4% formalin for 18 h before decalcification in ethylenediaminetetraacetic acid (EDTA) for 6 weeks. The specimens were then embedded in wax,

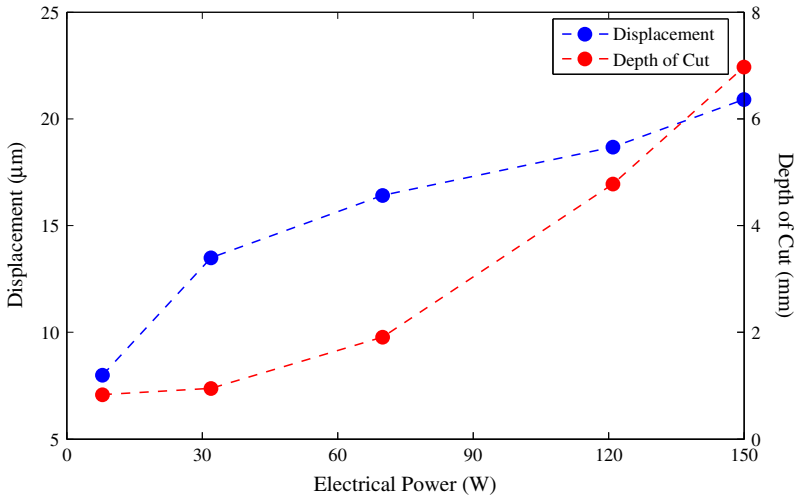

Fig. 8. UOSD electrical input power as a function of axial displacement of the end-cap (blue), and as a function of depth of cut (red), measured after 5 s of cutting. (For interpretation of the references to colour in this figure legend, the reader is referred to the web version of this article.)

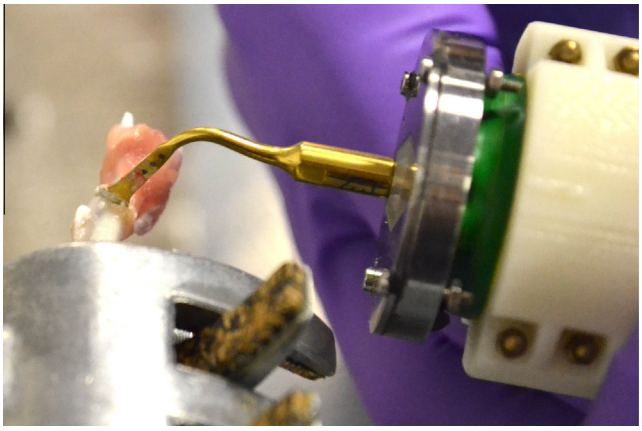

Fig. 10. Bone cutting using the UOSD.

sectioned and stained with haematoxylin and eosin (H&E). A histological examination was then performed around the cut site to identify live and dead cells, and their locations, as shown in Fig. 11.

Image analysis software (ImageJ) was used to record the position of the lacunae within the bone specimen where the cells (osteocytes) are found. This examination enabled the presence of the cell nuclei to be determined, indicating if the cell was alive or dead. The slide was split into regions of 50 μm from the cut surface. In each region, the quantity of both live and dead cells was recorded and compared statistically using an analysis of variance (ANOVA). The live cell percentage data for each region, for cuts made with and without coolant, are shown in Fig. 12.

The results show that there is more than 50% cell death within 50 μm of the cut surface and this value is unaffected by the use of cooling. It is likely that the combination of vibratory cutting action and temperature increase at the cut site causes a high proportion of cell death, even when the site is being cooled during cutting. However, over the next 200 μm of bone, the temperature gradient is steeper for cutting with coolant, with temperature falling towards the threshold of necrosis, resulting in less cell death. Beyond 250 μm the heat generated at the cut site is not sufficient to result in cell death at this distance and the coolant is of no additional benefit.

The effect of the UOSD on cell death during cutting was compared with that found for a sagittal saw (Stryker UK), and a manual

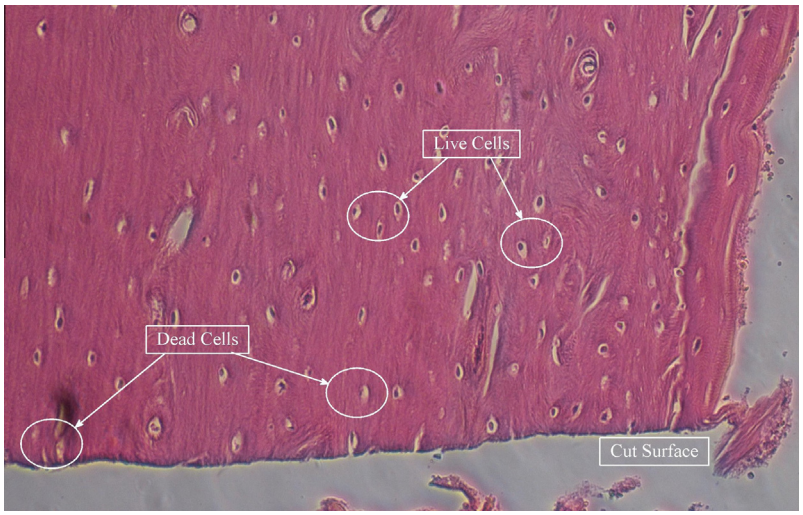

Fig. 11. The H&E stained section which shows sites of live and dead cells.

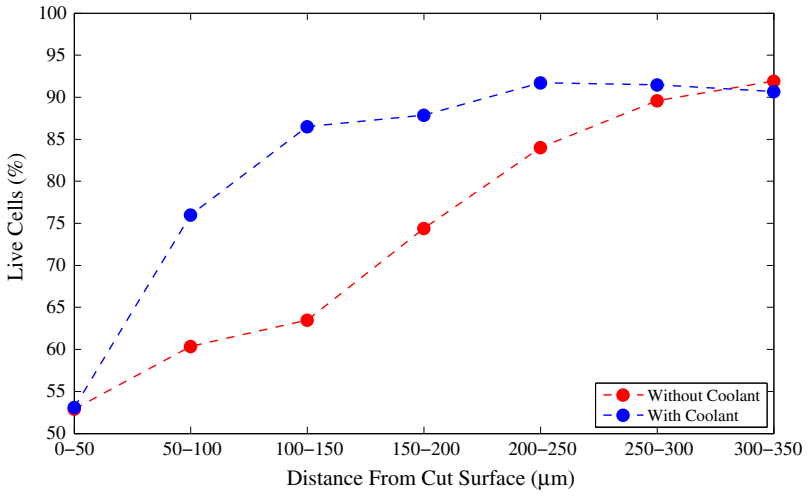

Fig. 12. Percentage of live cells at a distance from the cut surface for rat femurs cut by the UOSD, with and without the use of a coolant.

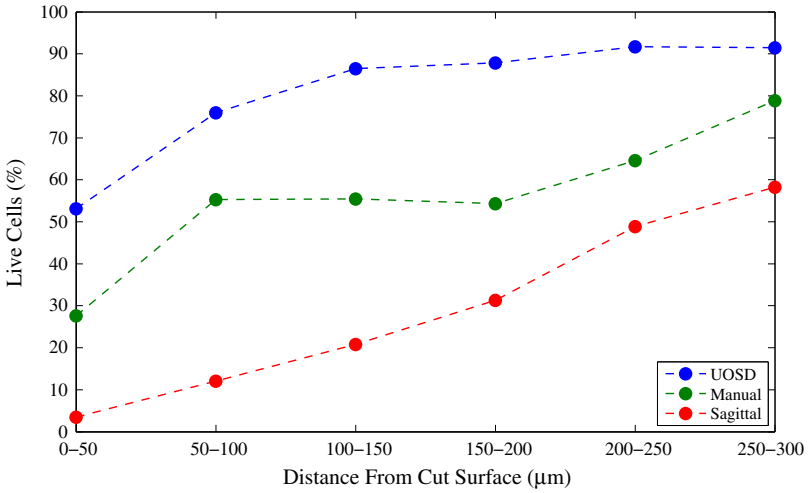

Fig. 13. Percentage of live cells at a distance from the cut surface for the UOSD, sagittal saw, and manual saw.

steel saw [24], all used to cut rat bone. The percentage of live cells was determined using the same histological methods outlined above, and the results of this analysis are shown in Fig. 13.

As can be seen in Fig. 13, the UOSD results in less cell death than both the manual and sagittal cutting tool. Analysis by ANOVA with Tukey correction reveals that the UOSD is statistically significantly different to both the manual and sagittal cutting tool from 0 to 200 μm ($p < 0.001$) and statistically significantly different to the sagittal saw at a distance of 200–250 μm ($p = 0.011$). No difference in cell death was found above 250 μm ($p = 0.55$).

Healing and new bone growth occurs due to cellular activity. In cases where fractured bones do not heal, known as non-union, one of the main causes is thought to be due to a fracture gap, or too large an area of biologically inert tissue [25]. By having a smaller zone of dead cells there is less risk of delayed healing or non-union occurring. This may be beneficial if ultrasonic devices can be used when performing bone cuts for orthopaedic implants, where more biologically active tissue close to the implant is known to encourage osteointegration.

5. Conclusions

In this research, an ultrasonic orthopaedic surgical device (UOSD) for bone surgery, based on an adaptation of the cymbal transducer for higher power applications, has been designed, fabricated, characterised and tested. The device assembly comprises a metal end-cap which is coupled to a back-shell, in which the piezoceramic disc is fixed in place. During operation, small radial vibrations of the piezoceramic disc are amplified by the end-cap, thereby producing a single radiating output face with sufficient axial amplitude to actuate an orthopaedic cutting blade. The geometry of the end-cap dictates the cavity resonance frequency of the SOFCym and the subsequent operating frequency of the UOSD is modified by the mass of the attached cutting insert. The back-shell geometry is critical for ensuring that flexural motions of the piezoceramic disc are avoided. A geometry is proposed that is effective for bone cutting at a frequency close to 25 kHz, with all the design analysis achieved through FEA. The end-cap is fabricated to incorporate a threaded stud, which enables the connection of a range of cutting inserts. The experimental characterisation of the device has demonstrated that a high level of correlation is achieved with the FEA estimations of modal frequency and mode shape. It is also shown that the UOSD exhibits weak nonlinear behaviour in the range of driving excitation levels, but can deliver sufficient ultrasonic displacement amplitude to cut bone, consistent with commercial devices. The added advantage is that this displacement amplitude is achieved with only one piezoceramic disc in a much smaller overall device.

Characterisation of the cutting performance demonstrated the potential of the UOSD, where precision cutting was achieved in animal bone, with a commercial cutting insert (Mectron S.p.A.) attached to the device. Bone cutting tests were conducted using the UOSD and the percentage of live/dead cells at a range of distances from the cut surface was compared with that found for a sagittal saw and a manual saw. Cuts performed with the UOSD resulted in significantly less cell death up to 250 μm from the cut surface compared with the currently used sagittal saw. The reduction in cell death has a clinical importance, since a higher number of living cells can improve healing after surgery.

Funding

This work has been funded by the Engineering and Physical Sciences Research Council (EPSRC) grant EP/G046948/1 with Mectron S.p.A., Carasco, Genoa, as project partner.

Authors' contributions

FB contributed to the drafting of the manuscript, the design and fabrication of the device, the data analysis, and the cutting experiments. AF contributed to the drafting of the manuscript, the design and fabrication of the device, and data analysis. RW contributed to the drafting of the manuscript and the assessment of cell survival, in addition to data analysis. ML and HS conceived the study, coordinated the investigation, and contributed to the drafting of the manuscript. All authors gave final approval for publication.

Acknowledgment

The authors would like to thank Mectron S.p.A. for providing the cutting inserts for this study.

References

[1] T. Arabaci, Y. Çiçek, C.F. Çanakç, Sonic and ultrasonic scalers in periodontal treatment: a review, Int. J. Dent. Hyg. 5 (1) (2007) 2–12, http://dx.doi.org/10.1111/j.1601-5037.2007.00217.x.

[2] N. Suppipat, Ultrasonics in periodontics, J. Clin. Periodontol. 1 (4) (1974) 206–213, http://dx.doi.org/10.1111/j.1600-051X.1974.tb01259.x.
[3] T. Aoki, S. Kaseda, Thoracoscopic resection of the lung with the ultrasonic scalpel, Ann. Thorac. Surg. 67 (4) (1999) 1181–1183, http://dx.doi.org/10.1016/S0003-4975(99)00134-4.
[4] M. Robiony, C.F. Polini, F. Costa, T. Vercellotti, M. Politi, Piezoelectric bone cutting in multipiece maxillary osteotomies, J. Oral. Maxillofac. Surg. 62 (6) (2004) 759–761, http://dx.doi.org/10.1016/j.joms.2004.01.010.
[5] Y. Watanabe, Y. Tsuda, E. Mori, A longitudinal-flexural complex-mode ultrasonic high-power transducer system with one-dimensional construction, Jpn. J. Appl. Phys. 32 (5B) (1993) 2430–2434, http://dx.doi.org/10.1143/JJAP.32.2430.
[6] H. Al-Budairi, M. Lucas, P. Harkness, A design approach for longitudinal–torsional ultrasonic transducers, Sens. Actuators A 198 (2013) 99–106, http://dx.doi.org/10.1016/j.sna.2013.04.024.
[7] A. Mathieson, A. Cardoni, N. Cerisola, M. Lucas, Understanding nonlinear vibration behaviours in high-power ultrasonic surgical devices, Proc. R. Soc. A 471 (2176) (2015) 1–19, http://dx.doi.org/10.1098/rspa.2014.0906.
[8] M.C. Catuna, Sonic energy: a possible dental application. Preliminary report of an ultrasonic cutting method, Ann. Dent. 12 (3) (1953) 100–101.
[9] L. Balamuth, K. Arthur, Ultrasonic cutting tool, US Patent 2,990,616, 1961.
[10] T. Vercellotti, Technological characteristics and clinical indications of piezoelectric bone surgery, Minerva Stomatol. 53 (5) (2004) 207–214.
[11] P. Leclercq, C. Zenati, S. Amr, D.M. Dohan, Ultrasonic bone cut part 1: state-of-the-art technologies and common applications, J. Oral Maxillofac. Surg. 66 (1) (2008) 177–182, http://dx.doi.org/10.1016/j.joms.2005.12.054.
[12] J. Zhang, W.J. Hughes, R.J. Meyer Jr., K. Uchino, R.E. Newnham, Cymbal array: a broadband sound projector, Ultrasonics 37 (8) (2000) 523–529, http://dx.doi.org/10.1016/S0041-624X(99)00111-0.
[13] Y. Sunny, C.R. Bawiec, A.T. Nguyen, J.A. Samuels, M.S. Weingarten, L.A. Zubkov, P.A. Lewin, Optimization of un-tethered, low voltage, 20–100 kHz flexural transducers for biomedical ultrasonics applications, Ultrasonics 52 (7) (2012) 943–948, http://dx.doi.org/10.1016/j.ultras.2012.03.004.
[14] R.J. Meyer Jr., W.J. Hughes, T.C. Montgomery, D.C. Markley, R.E. Newnham, Design of and fabrication improvements to the cymbal transducer aided by finite element analysis, J. Electroceram. 8 (2) (2002) 163–174, http://dx.doi.org/10.1023/A:1020512231158.
[15] P. Ochoa, J.L. Pons, M. Villegas, J.F. Fernandez, Effect of bonding layer on the electromechanical response of the cymbal metal-ceramic piezocomposite, J. Eur. Ceram. Soc. 27 (2–3) (2007) 1143–1149, http://dx.doi.org/10.1016/j.jeurceramsoc.2006.05.022.
[16] S. Lin, An improved cymbal transducer with combined piezoelectric ceramic ring and metal ring, Sens. Actuators A 163 (1) (2010) 266–276, http://dx.doi.org/10.1016/j.sna.2010.06.022.
[17] F. Bejarano, A. Feeney, M. Lucas, A cymbal transducer for power ultrasonics applications, Sens. Actuators A 210 (2014) 182–189, http://dx.doi.org/10.1016/j.sna.2014.02.024.
[18] F. Bejarano, Miniature ultrasonic bone cutting device based on a cymbal transducer, PhD thesis, University of Glasgow, 2014.
[19] F. Bejarano, M. Lucas, R. Wallace, A.M. Spadaccino, H. Simpson, Ultrasonic cutting device for bone surgery based on a cymbal transducer, Phys. Procedia. 63 (2015) 120–126, http://dx.doi.org/10.1016/j.phpro.2015.03.020.
[20] J.F. Tressler, W. Cao, K. Uchino, R.E. Newnham, Finite element analysis of the cymbal-type flextensional transducer, IEEE Trans. Ultrason. Ferr. Freq. Contr. 45 (5) (1998) 1363–1369, http://dx.doi.org/10.1109/58.726463.
[21] M.R. Rani, K. Prakasan, R. Rudramoorthy, Studies on thermo-elastic heating of horns used in ultrasonic plastic welding, Ultrasonics 55 (2015) 123–132, http://dx.doi.org/10.1016/j.ultras.2014.07.005.
[22] J.-L. Beziat, J.-C. Bera, B. Lavandier, A. Gleizal, Ultrasonic osteotomy as a new technique in craniomaxillofacial surgery, Int. J. Oral. Maxillofac. Surg. 36 (6) (2007) 493–500, http://dx.doi.org/10.1016/j.ijom.2007.01.012.
[23] A. Feeney, M. Lucas, Smart cymbal transducers with nitinol end caps tunable to multiple operating frequencies, IEEE Trans. Ultrason. Ferr. Freq. Contr. 61 (10) (2014) 1709–1719, http://dx.doi.org/10.1109/TUFFC.2013.006231.
[24] R.J. Wallace, A. Spadaccino, A. Leung, Z. Pan, O. Ganilova, A. Muir, M. Lucas, A.H. R.W. Simpson, A comparison of past, present and future bone surgery tools, Int. J. Orthop. 2 (3) (2015) 266–269.
[25] H.C. Brownlow, A.H.R.W. Simpson, Metabolic activity of a new atrophic nonunion model in rabbits, J. Orthop. Res. 18 (3) (2000) 438–442.